Macrophage-Derived Extracellular Vesicles as Drug Delivery Systems for Triple Negative Breast Cancer (TNBC) Therapy

Matthew J. Haney[1,2] · Yuling Zhao[1,2] · Yeon S. Jin[2] · Samuel M. Li[2] · Juli R. Bago[2] · Natalia L. Klyachko[1,2,3] · Alexander V. Kabanov[1,2,3] · Elena V. Batrakova[1,2]

Received: 30 July 2019 / Accepted: 27 September 2019 / Published online: 13 November 2019

Abstract
Efficient targeted delivery of anticancer agents to TNBC cells remains one of the greatest challenges to developing therapies. The lack of tumor-specific markers, aggressive nature of the tumor, and unique propensity to recur and metastasize make TNBC tumors more difficult to treat than other subtypes. We propose to exploit natural ability of macrophages to target cancer cells by means of extracellular vesicles (EVs) as drug delivery vehicles for chemotherapeutic agents, paclitaxel (PTX) and doxorubicin (Dox). We demonstrated earlier that macrophage-derived EVs loaded with PTX (EV-PTX) and Dox (EV-Dox) target cancer cells and exhibited high anticancer efficacy in a mouse model of pulmonary metastases. Herein, we report a manufacture and characterization of novel EV-based drug formulations using different loading procedures that were optimized by varying pH, temperature, and sonication conditions. Selected EV-based formulations showed a high drug loading, efficient accumulation in TNBC cells in vitro, and pronounced anti-proliferation effect. Drug-loaded EVs target TNBC in vivo, including the orthotopic mouse T11 tumors in immune competent BALB/C mice, and human MDA-MB-231 tumors in athymic nu/nu mice, and abolished tumor growth. Overall, EV-based formulations can provide a novel solution to a currently unmet clinical need and reduce the morbidity and mortality of TNBC patients.

Keywords Doxorubicin · Drug delivery systems · Extracellular vesicles · Paclitaxel · Triple negative breast cancer

Introduction

TNBC is a highly aggressive and metastatic cancer that is characterized by minimal estrogen and progesterone receptors, as well as nominal human epidermal growth factor receptor 2 (HER2) expression (Mersin, Yildirim et al. 2008). The development, progression, and metastasis of TNBC are the leading cause among female mortality. The current standard of care revolves around the use of various neoadjuvant chemotherapeutics (Ren, Hao et al. 2019), including anthracyclines, taxanes, and platinum agents (Walsh, Shalaby et al. 2019), as well as poly(ADP-ribose) polymerases (PARP) inhibitors (Zhou, Ji et al. 2016), and immune checkpoint inhibitors (Cyprian, Akhtar et al. 2019). Chemotherapy remains the only adjuvant treatment for TNBC, but responses are usually brief and associated with progressive resistance, short survival, and systemic toxicities. Thus, the development of new effective delivery approaches and in particular, more effective chemotherapies, determines translational success of these antineoplastic drugs for TNBC.

A large proportion of chemotherapeutics have low aqueous solubility, consequently requiring the use of specialized nanosized delivery vehicles (e.g. micelles, liposomes, polymeric nanoparticles, or other types of nanoparticles) for parenteral administration. Much effort has been dedicated to the development of drug nanoformulations targeted to tumors, but these efforts have been met with limited success (Chandolu and Dass 2013). Nanoparticles are promising platforms for treating cancer, but mainstream nanoparticles target tumors

Electronic supplementary material The online version of this article (https://doi.org/10.1007/s11481-019-09884-9) contains supplementary material, which is available to authorized users.

✉ Elena V. Batrakova
batrakov@ad.unc.edu; batrakov@email.unc.edu

[1] Center for Nanotechnology in Drug Delivery, University of North Carolina at Chapel Hill, Chapel Hill, North Carolina, USA

[2] UNC Eshelman School of Pharmacy, University of North Carolina at Chapel Hill, Chapel Hill, North Carolina 27599-7362, USA

[3] Deparment of Chemical Enzymology, Faculty of Chemistry, M.V. Lomonosov Moscow State University, Moscow, Russia

passively through the enhanced permeability and retention (EPR) effect, hence their accumulation in tumors is not efficient (typically <5% of the injected dose) and greatly affected by the tumor type and stage. A fundamental roadblock in the use of drug nanoformulations for many diseases is the opsonization of drug-loaded nanoparticles in the bloodstream and rapid drug clearance by mononuclear phagocyte system (MPS) (Peng, Zhang et al. 2013). To solve this problem, drug-loaded nanocarriers were decorated with a polyethylene glycol (PEG) corona to avoid this clearance, but along with the decreasing drug uptake by monocytes, the PEGylation concurrently reduced the interaction with target cancer cells, thus decreasing drugs therapeutic efficiency (Beckman, Minor et al. 1988, Yoshida, Burton et al. 1992, Veronese, Caliceti et al. 2002). Furthermore, as many as 30% of healthy recipients have already developed immune response to the PEG corona that significantly increases clearance of PEGylated drug nanocarriers (Dams, Laverman et al. 2000, Maeda et al. 2003, Masuda et al. 2003, Kashima et al. 2008). In this regard, active cancer-targeting moieties, such as antibodies and specific peptides, have been added to the drug nanoformulations, however the relatively short circulation time and the complexity of producing such carriers hinder their application. This approach is especially challenging taking into account the absence of specific markers on TNBC tumors. Finally, development of chronic autoimmune diseases such as rheumatoid arthritis was reported in a response to administration of different types of nanoparticles (Farhat, Silva et al. 2011, Mohamed, Verma et al. 2012). Therefore, engineering new clinically applicable drug delivery systems for TNBC therapy is of particular importance.

Recently, EVs have begun to be explored for use as drug delivery vehicles for non-native therapeutics such as nucleic acids (Alvarez-Erviti, Seow et al. 2011, Pan et al., 2012, Wahlgren et al., 2012, Shtam et al., 2013, Chen et al., 2014, Johnsen et al., 2014, Lamichhane et al., 2015, Aryani and Denecke 2016), therapeutic proteins (Haney et al., 2015), and small molecule drugs (Sun et al., 2010, Zhuang et al., 2011, Johnsen et al., 2014, Kalani et al., 2014, Tian et al., 2014, Agrawal et al., 2017, Schindler et al. 2019), as well as imaging agents (Gorgens et al. 2019). In fact, EVs naturally function as intracellular messengers, carrying RNAs and proteins between the cells (Mathivanan et al. 2010, Raposo and Stoorvogel 2013). Thus, EVs also exhibit increased stability in the blood that allows them to travel long distances within the body under both physiological and pathological conditions (Jiang and Gao 2017). The membranotropic nature of EVs suggests that these drug carriers will be able fuse with cancer cell's membranes and deliver their toxic payload. This process is facilitated by the expression of various adhesive proteins (tetraspanins and integrins) on the surface of EVs (Mulcahy et al. 2014). Of note, EVs are able to avoid one of the main hurdles for nanoformulations, sequestration in endosomes, and deliver their intraluminal cargo into the cytosol of target cancer cells (Montecalvo et al. 2012, Schindler et al. 2019). In addition, allogenic EVs have an immune privileged status, which allows for decreased drug clearance by MPS (Ha et al. 2016). Specifically, immunocytes-derived EVs are known to express CD47 receptor (Kaur et al. 2014), which interacts with signal regulatory protein α (SIRPα), to produce a "don't eat me" signal in phagocytes (Gardai et al. 2005, Long and Beatty 2013). Finally, EVs nanocarriers were shown to reduce unwanted side effects, including cardiotoxicity (Schindler et al. 2019), hepatotoxicity and immunogenicity (Saleh et al. 2019). For example, it was reported that in contrast to other delivery methods for doxorubicin, EVs do not accumulate in the heart, thereby providing potential for limiting the cardiac side effects and improved therapeutic index (Schindler et al. 2019). These unique features make EVs an attractive option for use as drug delivery vehicles for TNBC treatment. More information can be found in recent excellent review articles (Maas et al. 2017, Armstrong and Stevens 2018, Liu and Su 2019, Pullan et al. 2019, Zhang et al. 2019).

One of the major impediments for using EVs as drug delivery vehicles is their efficient loading with therapeutic agents without significant alterations of the membrane structure and surface proteins. We reported earlier that macrophage-derived EVs can be loaded with low molecular chemotherapeutics, such as PTX and Dox (Kim, Haney et al. 2016), or therapeutic proteins, such as catalase (Haney et al. 2015) and brain-derived neurotrophic factor (BDNF) (Yuan et al. 2017), and then utilized as drug delivery vehicles to tumors, or/and inflamed brain tissues. Various methods of drug incorporation into EVs nanocarriers were utilized, including electroporation, extrusion, and saponin permeabilization of EVs membranes, as well as sonication and freeze-thaw cycles.

Regarding targeted drug delivery, macrophage-derived EVs possess an extraordinary ability to interact with and accumulate in cancer cells. We demonstrated earlier several-fold increases in EVs accumulation in murine Lewis Lung Carcinoma cells (3LL-M27) compared to synthetic nanocarriers, polymer-based nanoparticles or liposomes (Kim, Haney et al. 2016). Important, macrophage-derived EVs target cancer cells, as well as inflamed tissues, through LFA-1 protein expressed on their surface and intercellular adhesion molecule-1 (ICAM-1) that is overexpressed in the most cancer cells (Rufino-Ramos et al. 2017, Yuan et al. 2017, Kim, Haney et al. 2018) and specifically in TNBC cells (Guo et al. 2014). Therefore, the inflammation developed upon

tumor growth and overexpression of ICAM-1 on tumor endothelium (Guo et al. 2014) may promote targeted delivery of anticancer agents to TNBC tumors by macrophage-derived EVs. Based on these findings, we hypothesized that biomimetic EV-based drug delivery system will be capable of recognizing and targeting TNBC, and as such, deliver incorporated chemotherapeutic to the TNBC tumors.

Here we report the development of new EV-based formulations for TNBC therapy. Dox and PTX were selected as representatives of two types of potent chemotherapeutics that have highly hydrophilic or hydrophobic properties, respectively. Several methods for loading were tested, including drug incorporation into naïve EVs followed by their isolation from macrophage conditioned media, or through parental cells during EVs formation. A robust accumulation, and nearly complete co-localization of systemically administered EVs with TNBC cells was demonstrated in mouse orthotopic tumor models. Furthermore, a significant inhibition of tumor growth was observed in both the orthotopic T11 tumors in immune competent BALB/C mice, and human MDA-MB-231 tumors in xenograft model in athymic nu/nu mice. We posit that EV-based formulations have a tremendous potential for efficient drug transport capable of overcoming various biological barriers. These formulations represent the next generation of drug delivery systems for precision medicine that can provide advantages of both cell-based drug delivery and nanotechnology.

Materials and Methods

Reagents

PTX and Dox was purchased from LC Laboratories (Woburn, MA, USA). Lipophilic fluorescent dyes, 1,1′-dioctadecyl-3,3,3′,3′-tetramethylindo-carbocyanine perchlorate (DIL), and were purchased from Invitrogen (Carlsbad, CA, USA). 4′,6-diamidino-2-phenylindole dihydrochloride (DAPI), and Triton X-100 were obtained from Sigma-Aldrich (St. Louis, MO, USA). Cell culture medium and fetal bovine serum (FBS) were purchased from Gibco Life Technologies, (Grand Island, NY, USA). Fluorescent polystyrene nanoparticles (Fluoro-Max G100), as well as Oregon Green™ 488 paclitaxel were obtained from Thermo Fisher Scientific (Waltham, MA, USA).

Cells

Murine TNBC cell line T11, and the human breast cancer cell lines MDA-MB-231 were obtained from the American Type Culture Collection (ATCC, Manassas, Virginia, USA), and grown in alpha Minimum Essential Medium (alpha-MEM, Mediatech, Tewksbury, MA, USA) containing 10% FBS, supplemented with 0.1 mM nonessential amino acids, 1 mM sodium pyruvate and 0.01 mg/mL bovine insulin (CellGro, Newington, USA), 10 mM HEPES, 50 μg/ml gentamycin (Invitrogen, Carlsbad, CA, USA). RAW 264.7 macrophages were purchased from ATCC and cultured in Dulbecco's modified Eagle's medium (DMEM) high glucose (Gibco) supplemented with 10% heat-inactivated fetal bovine serum (FBS), 1% penicillin and streptomycin. All cells were cultured in a humidified atmosphere at 37 °C and 5% CO_2.

Animals

Athymic nu/nu mice and Balb/C mice (6- to 8-weeks-old females) were obtained from Charles River Laboratories (Durham, NC, USA) and used for in vivo tumor assays. The animals were kept five per cage with an air filter cover under light- (12-h light/dark cycle) and temperature-controlled (22 ± 1° C) environment. Food and water were given ad libitum. All manipulations with the animals were performed under a sterilized laminar hood. All experiments were carried out with approval of Institutional Animal Care and Use Committees (IACUC) of University of North Carolina at Chapel Hill, in compliance with the US Public Health Service guidelines for the care and use of animals in research.

Isolation and Characterization of EVs

EVs were harvested from the conditioned media of RAW 264.7 macrophages seeded into Bioreactor (3.6×10^8 cells/flask) and cultured in EV-depleted media for 2 days using gradient centrifugation and described in (Haney et al. 2015). In brief, the culture supernatants were cleared of cell debris and large vesicles by sequential centrifugation at 300 g for 10 min, 1000 g for 20 min, and 10,000 g for 30 min, followed by filtration using 0.2 μm syringe filters. Then, the cleared sample was spun at 100,000 g for one hour to pellet the EVs, and supernatant was collected. The collected EVs (10^{11}–10^{12} EVs/flask) were washed twice with phosphate buffer solution (PBS). To avoid contamination by the FBS-derived EVs, FBS was spun at 100,000 g for 2 h to remove EVs before the experiment. The recovery of EVs was estimated by measuring the protein concentration using the Bradford assay and by Nanoparticle Tracking Analysis (NTA). The obtained EV fraction was re-suspended in PBS (500 μl, 1 mg/mL total protein), and characterized by western blot (Wes), Nanoparticle Tracking Analysis (NTA), Dynamic Light Scattering (DLS), Transmission Electron Microscopy (TEM) as described previously (Haney et al. 2015). EVs suspension was stored in aliquots at -80° C before use.

Drug Loading into EVs

Dox and PTX have different solubility in water solutions, therefore two separate types of methods for loading into EVs were carried out, *Type I* for Dox, and *Type II* for PTX.

Type I. In case of hydrophilic Dox, five different approaches were utilized: A stock solution of Dox (1 mg/mL) in 100 μL water was added to 100 μL EVs (4×10^{12} particles/mL) and incubated at RT for 2 h (**1**), or sonicated in water bath for 30 min and then incubated at RT for 1.5 h (**2**). The same mixture EVs and Dox was prepared in phosphate buffer (pH 8.0), incubated for 2 h at RT (**3**), or sonicated in water bath for 30 min and then incubated at RT for 1.5 h (**4**). Followed the incubation the mixtures were supplemented with 350 μL HEPES buffer (pH 7.4), and the excess free drug was separated from EV-Dox by size exclusion chromatography using a NAP-10 Sephadex G25 column (GE Healthcare, Buckinghamshire, UK). Finally, parental macrophages grown on 75 T flask were supplemented with 10 mL Dox solution in full media (30 μg/mL) and incubated for 4 h at 37 °C. Followed incubation, culture media was collected and EVs were isolated as described above (**5**). The loading efficiency of Dox in EVs formulation was determined by Dox fluorescence.

Type II. In case of hydrophobic PTX, another four different approaches were utilized. (**1**) PTX stock solution (1 mg/mL) in EtOH (10 μL) was placed into Eppendorf tube and EtOH was evaporated under nitrogen flow to form a thin film. Lyophilized EVs (3×10^{11} particles/100 μL) re-suspended in 30 μL water were added to the Eppendorf with PTX film and incubated for 1 h at 37 °C. (**2**) PTX stock solution (1 mg/mL) in ethanol (EtOH, 10 μL) was added to lyophilized EVs (3×10^{11} particles/100 μL) re-suspended in 30 μL water, and incubated for 1 h at 37 °C. (**3**) PTX stock solution (1 mg/mL) in EtOH (100 μL) was supplemented with 300 μL EVs in PBS (3×10^{11} particles/mL), and sonicated using probe sonicator (3 s "on"/3 s "off" at 100 W amplitude on ice, × 12 cycles). (**4**) PTX stock solution (1 mg/mL) in EtOH (100 μL) was supplemented with 300 μL EVs in PBS (3×10^{11} particles/mL), and sonicated using probe sonicator (3 s "on"/3 s "off" at 100 W amplitude at RT, 10 min cooling × 12 cycles). After sonication, EV-PTX solution were incubated for 1 h at 37 °C to allow for recovery of EVs membrane. In all cases, the excess of free drug was separated from EV-PTX by size exclusion chromatography using a NAP-10 Sephadex G25 column (GE Healthcare, Buckinghamshire, UK). The amount of PTX loaded into EVs was determined by two different methods: (*i*) HPLC on a Nucleosil C18 reverse phase column with a flow rate of 1 mL/min, 55% / 45% acetonitrile/water mobile phase, at 30 °C as described in (Kim, Haney et al. 2018); and (*ii*) by fluorescence using Oregon Green PTX (ThermoFisher Scientific, Waltham, MA, USA). The fluorescense was measured at wl_{ex} = 495 nm, and wl_{em} = 525 nm. The size and concentration of EV-based drug formulations was characterized by NTA.

Transmission Electron Microscopy (TEM)

A drop of isolated EVs fraction with incorporated drugs in PBS was placed on Formvar®-coated copper grid (150 mesh, Ted Pella Inc., Redding, CA). The dried grid containing EVs were stained with vanadyl sulfate and visualized using a Philips 201 transmission electron microscope (Philips/FEI Inc., Briarcliff Manor, NY).

Preparation and Loading of Liposomes with Dox or PTX

Dox was loaded into liposomes using extrusion procedure as describer previously (Haney et al. 2015). Liposomes were prepared by reverse phase evaporation method. Briefly, 2 mg of phospholipids (phosphatidylcholine:PEG-PE (1,2-distearoyl-sn-glycero-3-phosphoethanolamine-N-[methoxy(polyethylene glycol)-2000] 95:5 wt/wt), were dissolved in 6 mL of chloroform: diisopropyl ether 1:1 mixture. PEG-PE was added for stabilization of liposomes. Then PTX in EtOH (10 μL) and 1 ml PBS were added to the mixture. Mixture was intensively vortexed and bath sonicated to form stable emulsion. Organic solvents were evaporated on rotary evaporator forming the liposome aqueous dispersion. 200–250 μl of Millipore water can be added at this point to the mixture in case some part of water was also evaporated. Evaporation was continued to get almost clear dispersion. Then volume was adjusted to 1 mL by addition of small amount of water. Dispersion was vortexed and bath sonicated to get clear solution. Liposomes were sequentially extruded 21 times through 200 nm polycarbonate filters using a hand extruder (Avanti) at 60 °C. In case of Dox-loaded liposomes, a stock solution of Dox (pH 8.0) was added before the extrusion to load into liposomes. Liposomes were purified by PEG precipitation remove not encapsulated drug.

Manufacture Fluorescently-Labeled Nanocarriers

A suspension of EVs in PBS (1 mL) was supplemented with 1 mM DID solution (40 μL) and incubated at 37C for 30 min in dark. In parallel, 1 mL liposomal suspension was supplemented with 40 μL DID (1 mM solution in DMSO), and incubated for 30 min at 37C. DID-labeled nanocarriers were purified from non-incorporated dye by size-exclusion

chromatography on Sepharose CL-4B at RT. Fluorescence levels were measured at $wl_{ex} = 644$, $wl_{cut\ off} = 665$, $wl_{em} = 675$. The size of the obtained DID-nanocarriers was measured by NTA (for liposomes: Size min = 111 ± 2.4 nm, Size mode 98 ± 4.7, conc. 9.2×10^{12} particles/mL; for EVs: Size min = 110.3 ± 1.6 nm, Size mode 100.2 ± 3.4, conc. 8.2×10^{12} particles/mL).

Accumulation of Drug-Loaded into EVs in Breast Cancer Cells In Vitro

Effect of EVs nanocarriers on accumulation of Dox and PTX incorporated into EVs was investigated in MDA-MB-231 cancer cells in comparison with liposomal Dox or PTX (Lipo-Dox and Lipo-PTX, respectively). For this purpose, cell monolayers grown on 96-weel plates were incubated with drug-loaded EVs or liposomes (7×10^9 particles/ml) at 37 °C and 5% CO_2 for 4 h. Fluorescently-labeled Oregon Green ™ 488 PTX was used for these studies. Followed incubation, the media was removed, and cells were washed 3x with PBS. Liposomes were loaded with the drug using extruder as described above. The cell suspension was then lysed and analyzed for drug content by fluorescence.

In a parallel experiment, MDA-MB-231 cell monolayers grown in chamber slides, were incubated with drug-loaded EVs or liposomes (7×10^9 particles/ml) at 37 °C for 4 h. Dox or fluorescently-labeled Oregon Green ™ 488 PTX was used for these studies. Following incubation, cells were washed 3X with PBS, and mounted on slides with DAPI nuclei staining. The images of the cells were examined by a confocal fluorescence microscopic system ACAS-570 and corresponding filter set.

In Vitro Cytotoxicity Assay

The in vitro antitumor efficacy of EV-PTX and EV-Dox was assessed using a standard MTT (3-(4,5-dimethyl-2-thiazolyl)-2,5-diphenyl-2-H-tetrazoliumbromide) assay with three cancer cell lines, and compared to Taxol as described earlier (Batrakova et al. 2010). Briefly, TNBC cells (MDA-MB-231) were seeded at 5000 cells/well in 100 μL of media in 96-well plates overnight. Various concentrations of differed EV-PTX formulations, or Taxol were added to cancer cells for 48 h at 37C, 5% CO2. Following the incubation, the cells were washed and incubated with MTT reagent as described in (Batrakova et al. 2006). The cytotoxic activity of PTX was then evaluated using a standard MTT assay (Ferrari et al. 1990). The absorbance at 570 nm was measured using a Shimadzu RF5000 fluorescent spectrophotometer. The survival values were determined in relation to control cells cultured in drug-free media. IC_{50} values for the potency of EV-based and liposomal drug formulations were obtained using GraphPadPrism. All experiments were repeated at least three times. SEM values were less than 10%.

Production of a Lentiviral Vector (LV) and Transduction of T11 Cells

To utilize bioluminescence and fluorescence imaging, T11 cells were transduced with lentiviral vectors encoding mCherry (GBM8FlmC) and firefly luciferase (FLuc) fusion protein. The viral construct also encoded for a puromycin resistance gene downstream of mCherry, which was introduced to enable for selection of nearly 100% positively transduced cells. Lentiviral vector was created by PCR amplification of the cDNA sequences for mCherry and FLuc from pEmCherry (Clontech) and pcDNA-Luciferase (Addgene) with restriction enzyme sequences that were engineered into the primers. To create the final constructs, mCherry was digested with BamHI/EcoV and FLuc was digested with EcoV/XhoI. The digested fragments were ligated into the BamHI/XhoI digested pTK402 LV transfer vector (a kind gift from Dr. Tal Kafri, The University of North Carolina at Chapel Hill). LV-mCherryFLuc viral vectors were packaged in T11 cells by transient transfection using the psPAX2 and pMD2.G (Addgene) packaging plasmids and following previously described protocols (Sena-Esteves et al. 2004). A robust expression of both the fluorescent and bioluminescent markers was observed, and no difference in proliferation was detected between modified and unmodified cells. These cells (8FlmC-FLuc-T11) were used for biodistribution and therapeutic efficacy studies.

Orthotopic TNBC Mouse Model

To establish orthotopic TNBC mouse model, MDA-MB-231 cells (100,000 cells/50 μL/mouse) were implanted to the mammary fat pad (left side) in nude/nude mice ($n = 5–7$ mice/group) as described above. Cells at a dose of 100,000 in culture medium (50 μL) were mixed with a 1:1 ratio of matrigel (BD Biosciences) and then implanted to the mammary fat pad. When the tumor size reached a size of about 50 mm^3, mice were randomly divided into groups and *i.v.* injected with different formulations of Dox or PTX or fluorescently-labeled nanocarriers.

Biodistribution of EVs and Cancer Cells Targeting in Mice with TNBC Tumors

Balb/C mice ($n = 4$) were inoculated orthotopically with 8FlmC-FLuc-T11 cells (0.8×10^6 cells/mouse in 50 μL of matrigel) and solid tumor were allowed to establish for 10–12 days. Twelve days following cancer cells *i.v.* injection, DID-labeled EVs isolated from autologous macrophages were administered via tail vein (*i.v.*), or intratumoral (*i.t.*), or

intraperitoneal (*i.p.*) route in a dose 10^{11} particles/100 μl to mice with established T11 solid tumors. Twenty-four hours later, mice were sacrificed, perfused, tumors were extracted and sectioned on a microtome at a thickness of 20 μm; nuclei were stained with DAPI (300 mM, 5 min). The images of tumor sections were examined by a confocal fluorescence microscopic system ACAS-570 and corresponding filter set and processed using ImageJ software.

Therapeutic Efficacy of EV-PTX against TNBC In Vivo

The antineoplastic effects of EV-PTX were evaluated in an orthotopic mouse models of TNBC including T11 tumors in immune competent BALB/C mice, and human MDA-MB-231 tumors in athymic nu/nu mice. For this purpose, mice with established TNBC solid tumors as described above were *i.v.* injected with EV-Dox (2.5 mg/kg) or EV-PTX (0.5 mg/kg) in 10^9 EVs/100 μl/mouse. The same doses of commercially available drug formulation (Doxil or Taxol), or saline were administered into control groups ($N = 7$). The drug formulations were given intravenously (*i.v.*) in a volume of 10 mL/kg on days 1, 4, 7, 10, and 14 after random group assignment. Tumor length (L) and width (W) were measured, and tumor weight (WR) was calculated twice a week as follows:

$$\mathrm{WR} = 1/2 \text{ x L x } \mathrm{W}^2$$

The data were expressed in relative weight (RW) calculated using the formula:

$$RW = W_i/W_o,$$

where W_o is the mean tumor weight at the beginning of treatment and W_i is the mean tumor weight at any subsequent time point. The rate of tumor inhibition was determined on day 18 after group assignment for T11 tumors and day 64 for MDA-MB-231 tumors using the following formula:

$$TI\ (\%) = (1 - RW_t/RW_c)\ x\ 100\%,$$

where RW_t and RW_c are relative weights in the treated and control groups, respectively. Both the RW and TI indexes were considered not measurable if at least one animal in the treated group died by the day of measurement (on 19 day for T11 bearing mice, and on 65 day for MDA-MB-231 bearing mice).

Statistical Analysis

For the all experiments, data are presented as the mean ± *S.E.M.* Tests for significant differences between the groups were performed using a t-test or one-way ANOVA with multiple comparisons (Fisher's pairwise comparisons) using GraphPad Prism 5.0 (GraphPad software, San Diego, CA). A minimum p value of 0.05 was chosen as the significance level.

Results

Manufacture and Characterization of EV-Dox and EV-PTX

Two chemotherapeutic agents, Dox and PTX, were selected as representatives of hydrophilic and hydrophobic small molecule antineoplastic agents, respectively. Based on their solubility in water solutions, different approaches for incorporation these drugs into macrophage-derived EVs were utilized.

EV-Dox formulations were prepared through (*i*) drug incorporation into naïve EVs isolated from parental macrophages using mild sonication in water bath, or incubation at room temperature (RT); or (*ii*) incubation parental macrophages with the drug followed by EVs isolation from the cells conditioned media. Regarding the first approach, we reported earlier that the efficient drug loading can be achieved, when EVs subjected to sonication treatment in the presence of the drug (Kim, Haney et al. 2016). Herein, we utilized this approach with additional pH manipulations: at pH 7.4 (physiological conditions) and pH 8.0 (near the pI for Dox that is 8.4). As expected, EVs sonication in the presence of Dox increased drug incorporation into EV nanocarriers (Fig. 1 a, black bars) compared to simple drug co-incubation with EVs at RT (Fig. 1 a, white bars). In addition, loading at pH 8.0 further increased amount of the drug loaded into EVs compared to loading at physiological pH 7.4 (Fig. 1 a). We hypothesized that partial discharge of Dox molecule might facilitate its diffusion across tight lipid bilayers of EVs membranes and therefore increase Dox loading. Of note, complete discharging of Dox molecule at pI 8.4 resulted in drug precipitation; therefore, we did not utilize these conditions in further experiments. Next, drug loading through parental macrophages also provided a considerable amount of Dox incorporated into EVs (Fig. 1 a). Nevertheless, the amount of Dox loaded through parental cells was significantly lesser than the drug incorporated into EVs by co-incubation and/or sonication. Of note, the size of EV-Dox nanoformulations was slightly increased compared to naïve EVs as detected by NTA (Fig. 1 b), especially upon sonication at pH 8.0, and loading through parental cells.

Next, PTX is a highly hydrophobic drug; therefore, it was first diluted in ethanol and then incorporated into EVs through incubation at RT, or sonication procedures (Fig. 1 c). For the loading by incubation method, the drug was introduced using two ways: (*i*) PTX ethanol solution was first added to the tube

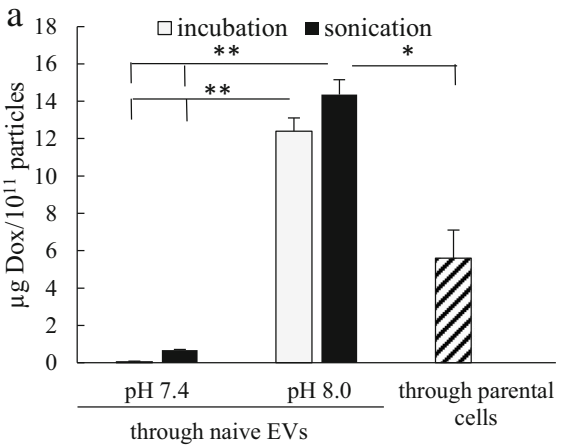

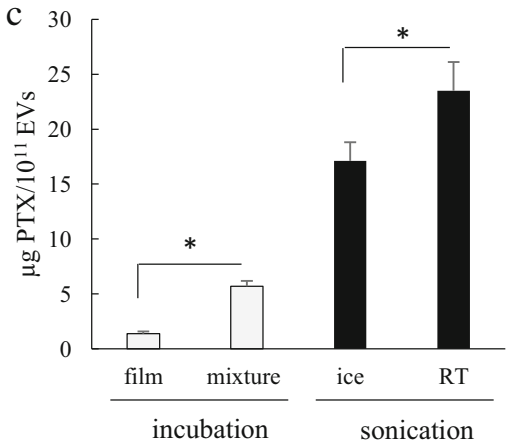

b

Formulation	Size mean, nm	Size mode, nm	Concentration particles/ml
Empty EVs	110.8 ± 4.1	100.0 ± 14.2	2.4 x 10^{12}
pH 7.4, incub.	123.0 ± 8.6	78.2 ± 2.6	1.3 x 10^{12}
pH 7.4, sonic.	128.0 ± 1.2	116.7 ± 15.9	2.7 x 10^{12}
pH 8.0, incub.	156.7 + 4.5	121.4 + 8.0	1.6 x 10^{12}
pH 8.0, sonic.	162.1 + 5.5	93.4 + 3.9	4.4 x 10^{12}
Cells loading	162.2 + 1.6	140.5 + 19.4	7.5 x 10^{12}

d

Formulation	Size mean, nm	Size mode, nm	Concentration particles/ml
Empty EVs	110.8 ± 4.1	100.0 ± 14.2	2.4 x 10^{12}
PTX, film	136.0 ± 9.4	98.5 ± 3.8	1.6 x 10^{12}
PTX, mix	142.7 ± 3.1	105.1 ± 4.0	2.4 x 10^{12}
Sonic/ice	164.4 + 8.8	120.3 + 13.6	2.0 x 10^{12}
Sonic/RT	129.4 + 2.3	102.4 + 7.5	1.3 x 10^{12}

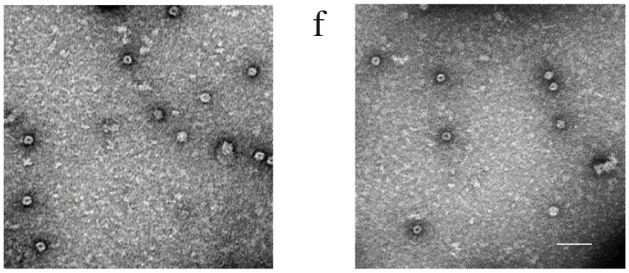

Fig. 1 Characterization of EVs-based drug formulations. **a**: Dox was loaded into naïve EVs at different pH (7.4 and 8.0, 2 h-incubation) or through parental macrophages (pH 7.4, 4 h-incubation). **c:** PTX was loaded into naïve EVs during incubation when drug was introduced as a thin film, or in the bulk solution; or sonication by probe sonicator (3 s "on"/3 s "off" at 100 W amplitude, 10 min cooling × 36 cycles) with or without cooling during sonication. **a:** Decreasing the overall charge of Dox molecule at pH 8.0 resulted in greater drug incorporation into EVs. **c:** Sonication at RT with periods of cooling down provided the most efficient loading into EVs, compared to sonication on ice at all times. Loading procedures slightly increased the size of EVs-based formulations for EV-Dox (**b**) and EV-PTX (**d**). TEM images revealed spherical shape and uniform size distribution of EV-Dox (**e**) and EV-PTX (**f**). *$p < 0.05$, **$p < 0.005$, $N = 6$. The bar = 200 nm

and ethanol was evaporated to obtain a thin film, and then EVs suspension was added to the PTX film; or (*ii*) PTX ethanol solution was directly added to the EVs suspension. The latter approach resulted in higher drug loading into EVs compared to thin film of PTX supplemented with EVs nanocarriers (Fig. 1 c). Furthermore, as expected, sonication of EVs in the presence of PTX provided the most efficient drug incorporation into EVs. Interesting, keeping the mixture on ice during the sonication procedure significantly reduced PTX loading compared to the mixture cooling only during the "off" time sonication periods. We hypothesized that elevated temperature during sonication might make EVs membranes less rigid, and therefore, increase their permeability for the drug. The obtained EV-PTX formulations were characterized by NTA (Fig. 1 d). Similar to EV-Dox (Fig. 1 b), NTA recorded slight increases in size of EV-PTX nanoformulations upon all loading procedures, especially for the sonication on ice.

TEM studies confirmed spherical morphology and relatively uniform size distribution of the drug-loaded EV-Dox and EV-PTX (Fig. 1 e and Fig. 1 f, respectively). Finally, according to Western blot analysis, sonicated EVs retained their EV-specific proteins, CD63, TSG101, and HSP90 (Figure S1 A), although at lesser levels than control naïve EVs (Figure S1 B).

Accumulation of EV-Dox and EV-PTX in Target Cancer Cells In Vitro

The efficient delivery of the drug payload into target cells is crucial for the therapeutic efficacy of EVs formulations. To have a fair comparison with EVs nanocarriers, we utilized liposomes that closely mimic natural cellular membranes. Specifically, cellular membranes contain abundant phospholipids, such as phosphatidylcholine (Reis et al.

2010). Therefore, we used a mixture of phosphatidylcholine and PEG-PE to resemble membrane bilayer. Herein, we compared accumulation of drugs incorporated into EVs against drugs loaded into liposomes, which also consist of lipid bilayers, ((phosphatidylcholine:PEG-PE (1,2-distearoyl-sn-glycero-3-phosphoethanolamine-N-[methoxy(polyethylene glycol)-2000] 95:5 wt/wt), but lack surface adhesion proteins, integrins and tetraspanins, that are present in EVs (Figure 1S). As expected, the chemotherapeutics loaded into EVs were taken up at much greater quantities by MDA-MB-231 cells than corresponding drugs loaded into synthetic nanocarriers, liposomes (ca. 150 times greater - for Dox, and 90 times - for PTX, Fig. 2 a). This is consistent with our previous reports, where we demonstrated that accumulation levels of fluorescently-labelled EVs nanocarriers in cancer 3LL-M27 cells was substantially greater then accumulation of liposomes or polysterol nanoparticles (Kim, Haney et al. 2016). Herein, we attribute increased drug accumulation to the adhesive proteins expressed on EVs surface, leading to the superior interactions with the cellular membranes compared to liposomes.

Finally, a superior intracellular accumulation of the incorporated into EVs anticancer drugs in TNBC cell monocytes was confirmed in confocal studies (Fig. 2 b). The incubation of MDA-MB-231 cells with EV-PTX and EV-Dox resulted in the considerable drug uiptake compared to liposomal-based drug formulations. Of note, significant amount of Dox was delivered to the target organelle, i.e. nuclei (Fig. 2 b).

Tumor Targeting and Biodistribution of EVs in Orthotopic TNBC Mouse Models

First, tumor accumulation of fluorescently-labeled DID-EVs was documented in nude mice with MDA-MB-231 solids upon systemic administration (Figrue S5). Interesting, EVs staining was more pronounced at the tumor periphery (Figure S5 B) compared to tumor center (Figure S5 A). We hypothesized that homogeneous intratumoral distribution of EVs nanocarriers may be limited by high interstitial pressure and dense stroma.

Next, we compared tumor accumulation of EVs and liposomes using immunocompetent orthotopic TNBC model upon different routes of administration. To induce tumors BALB/C mice were inoculated with T11 cells overexpressing mCherry reporter protein (mCherry-T11), and 15 days later when the tumors reached about 200 mm in diameter, the tumor-bearing mice were injected through intravenous (*i.v.),* or intraperitoneal (*i.p.),* or intratumoral (*i.t.)* routes with DID-labeled EVs or liposomes. Four hours after injections, mice were sacrificed, perfused; the tumors were sectioned on microtome and examined by confocal microscopy (Fig. 3). Confocal images revealed, a substantial amount of EVs administered through both *i.v.* and *i.p.* routes was accumulated in

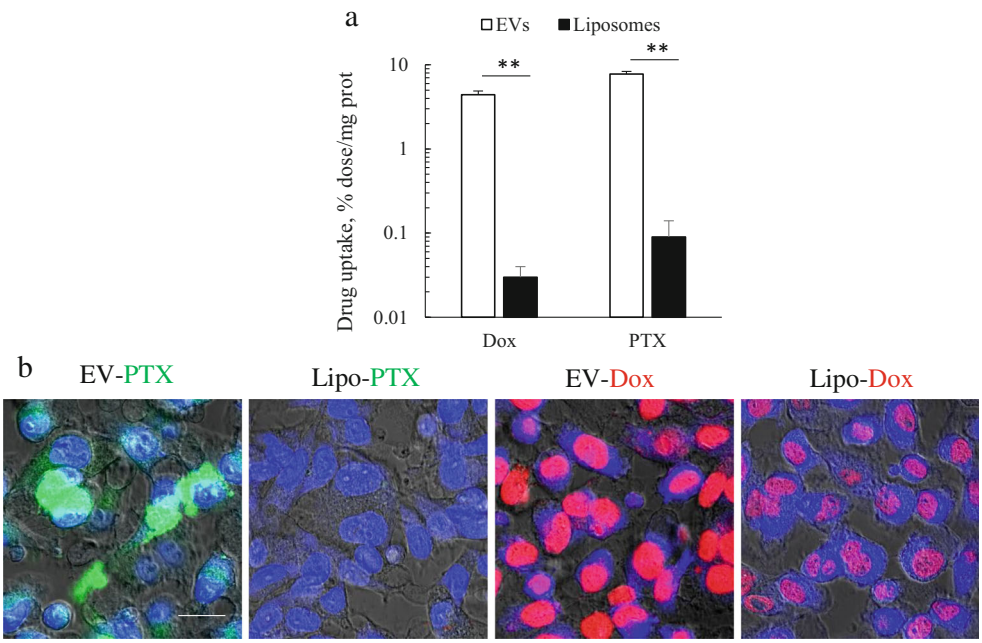

Fig. 2 EV-mediated accumulation of Dox and PTX in TNBC cells in vitro. EV-mediated accumulation of Dox and PTX in TNBC cells in vitro. MDA-MB-231 cell monolayers were supplemented with the selected optimal formulations of EV-Dox (pH 8.0, sonication), and EV-PTX (sonication at RT) or the same amount of liposomes loaded with Dox or fluorescently labeled PTX (7×10^{10} particles/mL) for 4 h, washed ×3 with PBS, and the amount of the accumulated drugs in the cells was accessed by fluorescence. **a**: EVs facilitated drug accumulation in TNBC cells at significantly greater levels compared to liposomes. $^{**}p < 0.005$. **b**: Confocal images confirmed the superior accumulation of PTX (green) or Dox (red) in cancer cells when loaded into EVs. Nuclei were labeled with DAPI (blue). The bar: 20 μm

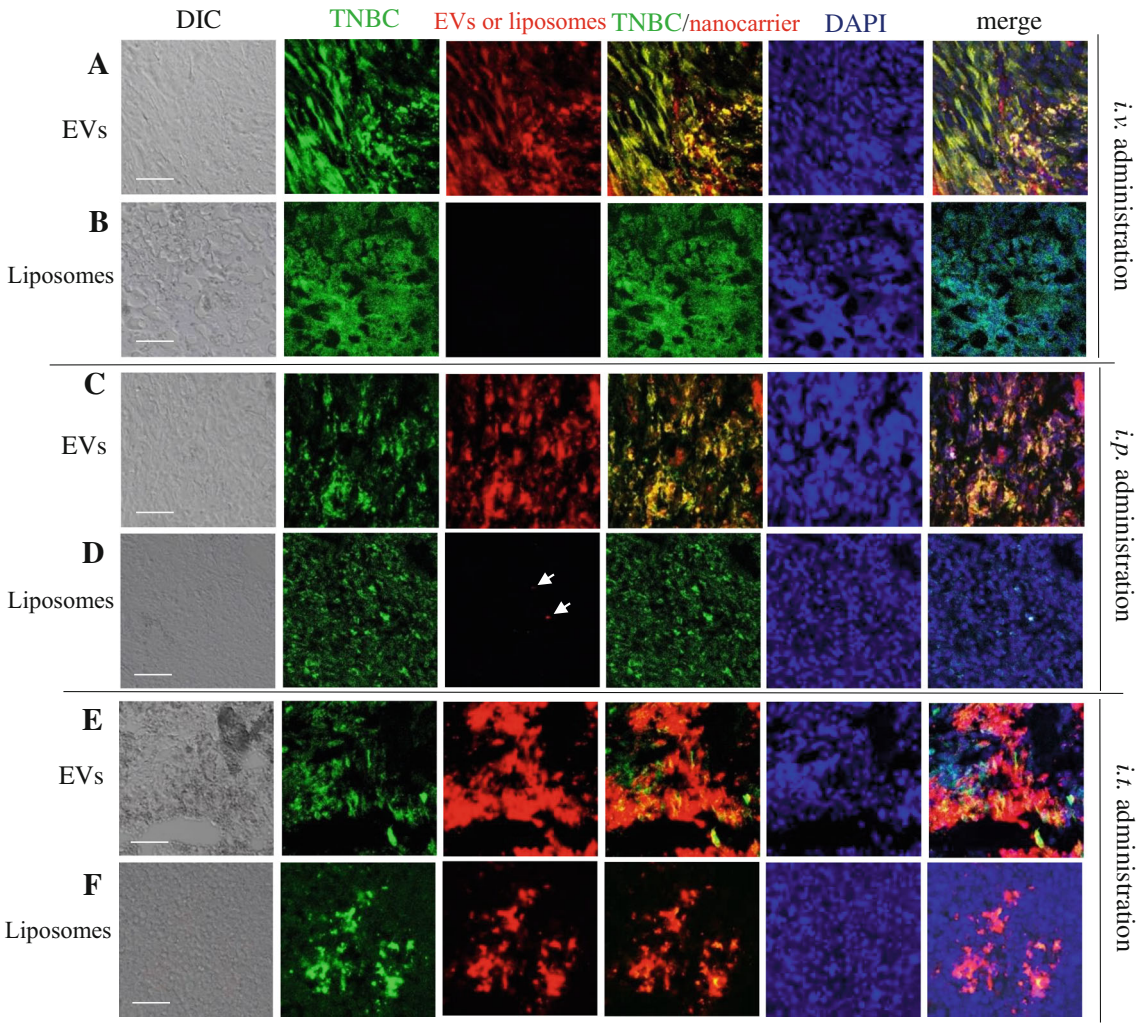

Fig. 3 DID-labeled EVs target TNBC solid tumors in vivo. BALB/C mice were orthotopically injected with 0.8×10^6 mCherry-T11 cells (here green) in matrigel. 15 days later, mice were injected with DID-EVs (**a**, **c**, **e**), or DID-liposomes (**b**, **d**, **f**) through *i.v.* (**a**, **b**), or *i.p.* (**c**, **d**), or *i.t.* (**e**, **f**) route (10^{11} particles/100 μL/mouse, here red). Four hours later, mice were sacrificed, perfused, tumor sides were sliced, sectioned, mounted on slides with DAPI staining (blue), and studied by confocal microscopy. Considerable amount of EVs, but not liposomes was detected in TNBC tumors upon *i.v.* and *i.p.* administration. A co-localization of EVs with TNBC cells was manifested in yellow (**a**, **c**, **e**). The bar = 50 μm

solid T11 tumors and co-localized with the cancer cells (Fig. 3 a, c). The estimates for co-localization of EVs with mCherry-T11 cells were 63.6 ± 2.1% and 48.4 ± 1.6% for of *i.v.* and *i.p.* administration routes, respectively. In contrast, little if any liposomes were delivered to the tumors followed by *i.v.* or *i.p.* administration (Fig. 3 b, d). Of note, after direct *i.t.* injection both EVs and liposomes were found in the tumors (Fig. 3 e, f). Additional images for EVs and liposome biodistribution in solid tumors are shown in Figures. S2, and S3, respectively. Moreover, similar to liposomes, fluorescently-labeled polymer-based nanocarriers (polystyrene nanoparticles, PS) also showed limited distribution in TNBC tumors upon *i.v.* and *i.p.* administration (Figure S4). Of note, no difference in EVs intratumoral distribution was found in T11 solids. The obtained data clearly demonstrated the advantages EVs over liposomes as drug nanocarriers suggesting that systemically administered EVs can successfully reach solid tumors and deliver their drug payload to target TNBC cells.

Table 1 Cytotoxicity of EV-PTX and EV-Dox

Formulation	$IC_{,50,}$ (μM)[1]
EVs alone	N/A
Dox	6.4 ± 0.7
Doxil	3.3 ± 0.05
EV-Dox	2.1 ± 0.03
Taxol	0.6 ± 0.03
EV-PTX	2.1 ± 0.03

[1] Data are shown as IC_{50} values in μM ± SD. Values are the mean of triplicate experiments

Therapeutic Effect of EV-Based Formulations against TNBC Tumors In Vitro and In Vivo

We selected optimized formulations of EV-Dox (pH 8, sonication) and EV-PTX (sonication at RT) with the highest loading efficiency, and examined their cytotoxicity in vitro using MDA-MB-231 cells. Consistently with previous reports (Kim, Haney et al. 2016, Kim, Haney et al. 2018), the incorporation of anticancer drugs into EVs did not significantly alter drug IC_{50} compared to commercially available drug formulations, Doxil and Taxol (Table 1), indicating that the incorporation of drugs into EVs does not decrease their ability to reach their intracellular targets and eradicate cancer cells.

Finally, for the in vivo efficacy studies, we used an immunodeficient (Fig. 4 a), and immunecompetent (Fig. 4 b) orthotopic TNBC tumor models. For the former, nude mice with established MDA-MB-231 solids were systemically (*i.v.*) injected with the optimal EV-PTX formulation (sonication at RT, 0.5 mg/kg), or the same dose of commercially available PTX formulation, Taxol, or empty EVs or saline as a control four times on day 1, 4, 7, and 9; and the tumor growth was recorded until the first animal in control group injected with saline reached an end point. A systemic administration of EV-PTX caused significantly stronger suppression of tumor growth ($TI = 71\%$) compared to the same dose of commercially available PTX formulation, Taxol ($TI = 29\%$). No significant anticancer effect was found for sham EVs (without PTX, $TI = 21\%$).

Next, immunocompetent Balb/C mice with established TNBC tumors were systemically (*i.v.*) injected with Dox in saline (2.5 mg/kg/mouse), or the same dose of optimized EV-Dox formulation (pH 8, sonication), or liposomal Dox (Doxil), or saline as a control. The incorporation of Dox into EVs resulted in significant inhibition of TNBC tumor growth in immune competent mice BALB/C mice (Fig. 4 b). Specifically, *TI* values were ca. 40%. In contrast, Dox alone did not have any significant antitumor activity in T11 solids ($TI = 19\%$). Noteworthy, injections of control empty (naïve) EVs without incorporated drugs did not slow down tumor growth in mice with orthotopic TNBC tumors (Fig. 4 a, b). Of note, liposomal Dox formulation also showed inhibition of tumor growth in this animal model that was not significantly different from EV-Dox inhibition effect. We hypothesized that accordingly to biodistribution studies, T11 solids may have relatively low-density stroma that allows deep penetration of Dox released from nanocarriers (EVs and liposomes) to the center of the tumor.

Discussion

The delivery of antineoplastic agents to cancer cells remains one of the greatest challenges for the treatment of TNBC. Several synthetic nanoformulations of small molecule anticancer drugs and antioxidants are being developed for treatment of TNBC (Greish et al. 2018, Krausz et al. 2018, Sorolla et al. 2019, Valcourt et al. 2019). However, conventional nanoparticles have limited biocompatibility, and normally are cleared rapidly from the circulation by the MPS (Peng et al. 2013). To address this problem, we developed a novel drug delivery system that is based on natural vectors EVs for the delivery of anticancer agents with different solubility in water. We utilized macrophage-derived EVs that exert unique

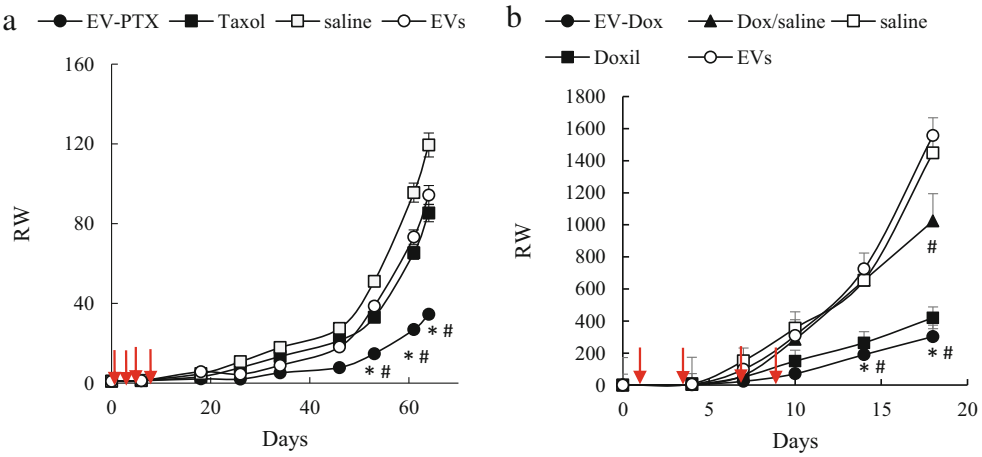

Fig. 4 EV-based formulations of PTX and Dox suppress tumor growth in orthotopic TNBC mouse models. **c**: nude mice bearing MDA-MB-231 solid tumors, or **b**: Balb/C mice bearing T11 solid tumors were injected on days 1, 4, 7, and 9 (red arrows) with: saline, or commercially available drug nanoformulation (Taxol or Doxil), or Dox in saline, or drug incorporated into EVs (EV-PTX or EV-Dox), and the relative tumor weight (RW) ± SEM, was determined for each group ($N = 7$). EV-based formulations of PTX and Dox showed superior therapeutic efficacy compared to Taxol (**a**), or Dox alone (**b**), or saline-treated animals. *$p < 0.05$ compared to Taxol or Dox-treated, and #$p <$ 0.05 compared to saline-treated animals

biological activity reflective of their origin, macrophages, specifically, target cancer cells in vivo.

Using EVs as drug delivery vehicles offers a number of benefits over common drug administration regimens; however, there are some limitations and challenges that need to be addressed. One of the major challenges is the efficient loading of EVs without significant alterations to the structure and content of the EV membranes. To achieve favorable conditions for drug loading, we developed a specific procedure wherein the relatively tight and highly structured lipid bilayers are reshuffled upon a mild sonication. One of the important conclusions regarding these evaluations is that a small molecule anticancer drug should be relatively hydrophobic to incorporate into EVs membranes. Thus, using pH that is close to pI for Dox (i.e. decreasing charge of the molecule and increasing its hydrophobicity) significantly improved Dox loading into EVs. On the other hand, PTX is a highly hydrophobic compound; therefore, the main challenge for the PTX incorporation is to provide a wide access of this drug to EVs membranes. According to our studies, the incorporation of PTX into EVs nanocarriers was more efficient when PTX was added to EVs suspension in ethanol solution, compared to PTX thin film. We hypothesized that the addition of the drug to the bulk solution along with the small amount of ethanol provided high local concentration of PTX, and at the same time, caused a mild fluidization of EVs membranes resulting in the efficient PTX incorporation. Another important finding is that the temperature of the mixture drastically affects the drug loading into EVs. Specifically, sonication EVs with PTX at room temperature (with short periods of cooling down in between the cycles) was more efficient that sonication on ice that was kept for the continuous time (during sonication and intermediate periods). Of note, Western blot analysis indicated that EV-based drug formulations obtained by sonication retain specific adhesive proteins in EVs membranes that are crucial for their interaction with target cancer cells.

Regarding delivery of anticancer agents to TNBC cells, EVs facilitated drug accumulation in cancer cells compared to liposomal-based drug nanoformulations in vitro. This is in agreement with a recent report regarding rapid cellular uptake of doxorubicin loaded into EVs by electroporation and its redistribution from endosomes to the cytoplasm and nucleus in a number of cultured and primary cell lines, when compared to free Dox, or liposomal Dox (Schindler et al. 2019).

The most promising results were obtained in the mouse TNBC models. Our data demonstrate a robust accumulation and significant co-localization of systemically administered EVs with TNBC cells upon different routes of administration, including *i.v., i.p.,* and *i.t.* administration. In contrast, little if any liposomes or polymer-based nanoparticles were found in TNBC solids upon *i.v.,* and *i.p.* administration. Only *i.t.* route allowed delivery of significant amount of these synthetic nanocarriers to the tumors. To this end, we reported earlier that macrophage-derived EVs inherited LFA1 protein expressed on EVs membranes that may be responsible for their preferential accumulation in cancer cells upon systemic administration (Kim, Haney et al. 2016, Kim, Haney et al. 2018). The investigations of trafficking of EVs and their components (loaded therapeutic agents, as well as EVs lipids, and proteins, etc.) are on the way in our laboratory.

Finally, a systemic administration of EV-based formulations of PTX and Dox resulted in the potent tumor growth suppression in mice with TNBC solids, as compared to Taxol or Dox treated animals, probably, due to the efficient delivery of the incorporated into EVs drug to tumors. Furthermore, low immunogenicity and high stability might increase EVs time circulation in the blood (Gardai et al. 2005, Long and Beatty 2013, Kaur et al. 2014, Ha et al. 2016, Jiang and Gao 2017). In fact, it is known that EV-mediated cell-to-cell communication is key in the battle between cancer and the immune system (Finn 2012). Thus, Parolini et al. (Parolini et al. 2009) showed that EVs fusion with target cells occurs more efficiently under acidic conditions, implying that EVs may be taken up preferentially by tumors (which have an acidic microenvironment) rather than the surrounding healthy tissue.

Overall, all three mechanisms mentioned here are likely to have significant impact on EV-based drug formulations anticancer activity, i.e.: (*i*) efficient delivery of incorporated cargo into target cancer cells, (*ii*) preferential accumulation in tumor cells due to LFA1/ICAM1 interactions, and (*iii*) prolonged circulation time in the blood. Further studies of the mechanism of these superior antineoplastic effects are ongoing in our lab.

Using EVs as drug delivery vehicles takes advantage of their natural carriage and extraordinary ability to interact with target cells. It offers several benefits over common drug administration regimens; however there are number of limitations and challenges that need to be addressed. One of the major challenges is whether the sufficient number of these nanocarriers can be generated (Nordin et al. 2015) to manufacture scalable and reproducible lots. The reproducibility and consistency of the product lots may be difficult to achieve as the starting material may come from many different donors and thus possesses inherent variability (Patel et al. 2005). As of today, the good manufacturing procedures (GMP) have been developed in Industry and Academia (Pachler et al. 2017, Mendt et al. 2018), such as Wake Forest Institute for Regenerative Medicine labs (EVs enriched with specific microRNAs). These efforts support more than half a dozen clinical trials that have already demonstrated feasibility and short-term safety of EVs administration (Mentkowski et al. 2018). Specifically, EVs were purified from monocyte cultures from 15 patients with advanced metastatic melanoma. The GMP process allowed harvesting about 5×10^{14} EVs MHC class II carriers (Mignot et al. 2006). In another trial, a total of 40 patients with advanced colorectal cancer received up to 2×10^{12} EVs weekly for 4 weeks (Dai et al. 2008).

The therapies were safe, feasible, and efficient in induction of antigen-specific T lymphocyte response. A major effort is underway on clinical implementation of EV-based therapeutics, including: (**1**) MolecuVax, Inc. (peptide/EVs technology); (**2**) Stem Cell Medicine Ltd. (EVs for neurodegenerative diseases); (**3**) Evox Therapeutics (EVs for Duchenne muscular dystrophy); and (**4**) Jazz Pharmaceuticals Inc. (EVs for cancer). The cellular origin for EVs varies from dendritic cells (Escudier et al. 2005, Morse et al. 2005, Besse et al. 2016, Baghaei et al. 2018), reticulocytes (Diaz-Varela et al. 2018), erythrocytes (Hafiane and Daskalopoulou 2018), monocytes (Singhto et al. 2018), macrophages (Rice et al. 2018) to mesenchymal (Bobis-Wozowicz et al. 2017, de Godoy et al. 2018, Ferreira and Gomes 2018) and human iPSCs (Adamiak et al. 2018, Taheri et al. 2018). Notably, EVs can be concentrated, lyophilized, and reconstituted in aqueous solutions (Haney et al. 2015). Thus, quality control of the lots is of paramount importance in order to ensure safety and reproducibility. In summary, EVs offer many advantages over other potential drug delivery systems, specifically: high stability, low immunogenicity, ability to avoid accumulation and clearance by mononuclear phagocytes, biocompatibility, extraordinary biological activity, and efficient drug transfer to target cells. These biomimetic drug delivery systems that are capable of recognizing and targeting cancer cells and inflammation, are one of the promising and competitive carriers for drug delivery, especially in case of TNBC tumors with low expression of specific proteins for targeted anticancer therapies available in clinic. In conclusion, EVs promise an unparalleled efficacy in the treatment of many life-threatening conditions, including those lacking effective pharmacotherapy.

Acknowledgments This study was supported by the Elsa U Pardee Foundation grant 17-4676 (to EVB), Eshelman Institute for Innovation grant UNC EII29-201 (to EVB), and the Russian Foundation for Basic Research (RFBR) grants 17-54-33027 and 18-29-09154 (to NLK). We would like to acknowledge the support of the UNC Nanomedicine Characterization Core Facility (http://ncore.web.unc.edu) in the EVs characterization.

Author Contributions EVB wrote and edited the manuscript. MJH and YZ contributed to the production of EVs used in these experiments. MJH, YZ, YSJ, SML, and JRB carried out experiments and contributed to data analysis. NLK and AVK contributed to the overall direction and coordination of the study as well as contributions to experimental design and data analysis.

Compliance with Ethical Standards

Conflict of Interest The authors have declared that no conflict of interest exists.

References

Adamiak M, Cheng G, Bobis-Wozowicz S, Zhao L, Kedracka-Krok S, Samanta A, Karnas E, Xuan YT, Skupien-Rabian B, Chen X, Jankowska U, Girgis M, Sekula M, Davani A, Lasota S, Vincent RJ, Sarna M, Newell KL, Wang OL, Dudley N, Madeja Z, Dawn B, Zuba-Surma EK (2018) Induced pluripotent stem cell (iPSC)-derived extracellular vesicles are safer and more effective for cardiac repair than iPSCs. Circ Res 122(2):296–309

Agrawal AK, Aqil F, Jeyabalan J, Spencer WA, Beck J, Gachuki BW, Alhakeem SS, Oben K, Munagala R, Bondada S, Gupta RC (2017) Milk-derived exosomes for oral delivery of paclitaxel. Nanomedicine 13(5):1627–1636

Alvarez-Erviti L, Seow Y, Yin H, Betts C, Lakhal S, Wood MJ (2011) Delivery of siRNA to the mouse brain by systemic injection of targeted exosomes. Nat Biotechnol 29(4):341–345

Armstrong JPK, Stevens MM (2018) Strategic design of extracellular vesicle drug delivery systems. Adv Drug Deliv Rev 130:12–16

Aryani A, Denecke B (2016) Exosomes as a Nanodelivery system: a key to the future of Neuromedicine? Mol Neurobiol 53(2):818–834

Baghaei K, Tokhanbigli S, Asadzadeh H, Nmaki S, Reza Zali M, Hashemi SM (2018) Exosomes as a novel cell-free therapeutic approach in gastrointestinal diseases. J Cell Physiol

Batrakova EV, Kelly DL, Li S, Li Y, Yang Z, Xiao L, Alakhova DY, Sherman S, Alakhov VY, Kabanov AV (2006) Alteration of genomic responses to doxorubicin and prevention of MDR in breast cancer cells by a polymer excipient: pluronic P85. Mol Pharm 3(2):113–123

Batrakova EV, Li S, Brynskikh AM, Sharma AK, Li Y, Boska M, Gong N, Mosley RL, Alakhov VY, Gendelman HE, Kabanov AV (2010) Effects of pluronic and doxorubicin on drug uptake, cellular metabolism, apoptosis and tumor inhibition in animal models of MDR cancers. J Control Release 143(3):290–301

Beckman JS, Minor RL Jr, White CW, Repine JE, Rosen GM, Freeman BA (1988) Superoxide dismutase and catalase conjugated to polyethylene glycol increases endothelial enzyme activity and oxidant resistance. J Biol Chem 263(14):6884–6892

Besse B, Charrier M, Lapierre V, Dansin E, Lantz O, Planchard D, Le Chevalier T, Livartoski A, Barlesi F, Laplanche A, Ploix S, Vimond N, Peguillet I, Thery C, Lacroix L, Zoernig I, Dhodapkar K, Dhodapkar M, Viaud S, Soria JC, Reiners KS, Pogge von Strandmann E, Vely F, Rusakiewicz S, Eggermont A, Pitt JM, Zitvogel L, Chaput N (2016) Dendritic cell-derived exosomes as maintenance immunotherapy after first line chemotherapy in NSCLC. Oncoimmunology 5(4):e1071008

Bobis-Wozowicz S, Kmiotek K, Kania K, Karnas E, Labedz-Maslowska A, Sekula M, Kedracka-Krok S, Kolcz J, Boruczkowski D, Madeja Z, Zuba-Surma EK (2017) Diverse impact of xeno-free conditions on biological and regenerative properties of hUC-MSCs and their extracellular vesicles. J Mol Med (Berl) 95(2):205–220

Chandolu V, Dass CR (2013) Treatment of lung cancer using nanoparticle drug delivery systems. Curr Drug Discov Technol 10(2):170–176

Chen L, Charrier A, Zhou Y, Chen R, Yu B, Agarwal K, Tsukamoto H, Lee LJ, Paulaitis ME, Brigstock DR (2014) Epigenetic regulation of connective tissue growth factor by MicroRNA-214 delivery in exosomes from mouse or human hepatic stellate cells. Hepatology 59(3):1118–1129

Cyprian FS, Akhtar S, Gatalica Z, Vranic S (2019) Targeted immunotherapy with a checkpoint inhibitor in combination with chemotherapy: a new clinical paradigm in the treatment of triple-negative breast cancer. J Basic Med Sci, Bosn

Dai S, Wei D, Wu Z, Zhou X, Wei X, Huang H, Li G (2008) Phase I clinical trial of autologous ascites-derived exosomes combined with GM-CSF for colorectal cancer. Mol Ther 16(4):782–790

Dams ET, Laverman P, Oyen WJ, Storm G, Scherphof GL, van Der Meer JW, Corstens FH, Boerman OC (2000) Accelerated blood clearance and altered biodistribution of repeated injections of sterically stabilized liposomes. J Pharmacol Exp Ther 292(3):1071–1079

de Godoy MA, Saraiva LM, de Carvalho LRP, Vasconcelos-Dos-Santos A, Beiral HJV, Ramos AB, Silva LRP, Leal RB, Monteiro VHS,

Braga CV, de Araujo-Silva CA, Sinis LC, Bodart-Santos V, Kasai-Brunswick TH, Alcantara CL, Lima A, da Cunha ESNL, Galina A, Vieyra A, De Felice FG, Mendez-Otero R, Ferreira ST (2018) Mesenchymal stem cells and cell-derived extracellular vesicles protect hippocampal neurons from oxidative stress and synapse damage induced by amyloid-beta oligomers. J Biol Chem 293(6):1957–1975

Diaz-Varela M, de Menezes-Neto A, Perez-Zsolt D, Gamez-Valero A, Segui-Barber J, Izquierdo-Useros N, Martinez-Picado J, Fernandez-Becerra C, Del Portillo HA (2018) Proteomics study of human cord blood reticulocyte-derived exosomes. Sci Rep 8(1): 14046

Escudier B, Dorval T, Chaput N, Andre F, Caby MP, Novault S, Flament C, Leboulaire C, Borg C, Amigorena S, Boccaccio C, Bonnerot C, Dhellin O, Movassagh M, Piperno S, Robert C, Serra V, Valente N, Le Pecq JB, Spatz A, Lantz O, Tursz T, Angevin E, Zitvogel L (2005) Vaccination of metastatic melanoma patients with autologous dendritic cell (DC) derived-exosomes: results of thefirst phase I clinical trial. J Transl Med 3(1):10

Farhat SC, Silva CA, Orione MA, Campos LM, Sallum AM, Braga AL (2011) Air pollution in autoimmune rheumatic diseases: a review. Autoimmun Rev 11(1):14–21

Ferrari M, Fornasiero M, Isetta A (1990) MTT colorimetric assay for testing macrophage cytotoxic activity in vitro. J Immunol Methods 131(2):165–172

Ferreira ADF, Gomes DA (2018) Stem cell extracellular vesicles in skin repair. Bioengineering (Basel) 6(1)

Finn, O. J. (2012). "Immuno-oncology: understanding the function and dysfunction of the immune system in cancer." Ann Oncol 23 Suppl 8: viii6-9

Gardai SJ, McPhillips KA, Frasch SC, Janssen WJ, Starefeldt A, Murphy-Ullrich JE, Bratton DL, Oldenborg PA, Michalak M, Henson PM (2005) Cell-surface calreticulin initiates clearance of viable or apoptotic cells through trans-activation of LRP on the phagocyte. Cell 123(2):321–334

Gorgens A, Bremer M, Ferrer-Tur R, Murke F, Tertel T, Horn PA, Thalmann S, Welsh JA, Probst C, Guerin C, Boulanger CM, Jones JC, Hanenberg H, Erdbrugger U, Lannigan J, Ricklefs FL, El-Andaloussi S, Giebel B (2019) Optimisation of imaging flow cytometry for the analysis of single extracellular vesicles by using fluorescence-tagged vesicles as biological reference material. J Extracell Vesicles 8(1):1587567

Greish K, Pittala V, Taurin S, Taha S, Bahman F, Mathur A, Jasim A, Mohammed F, El-Deeb IM, Fredericks S, Rashid-Doubell F (2018) Curcumin(−)copper complex nanoparticles for the management of triple-negative breast Cancer. Nanomaterials (Basel) 8(11)

Guo P, Huang J, Wang L, Jia D, Yang J, Dillon DA, Zurakowski D, Mao H, Moses MA, Auguste DT (2014) ICAM-1 as a molecular target for triple negative breast cancer. Proc Natl Acad Sci U S A 111(41): 14710–14715

Ha D, Yang N, Nadithe V (2016) Exosomes as therapeutic drug carriers and delivery vehicles across biological membranes: current perspectives and future challenges. Acta Pharm Sin B 6(4):287–296

Hafiane A, Daskalopoulou SS (2018) Extracellular vesicles characteristics and emerging roles in atherosclerotic cardiovascular disease. Metabolism 85:213–222

Haney MJ, Klyachko NL, Zhao Y, Gupta R, Plotnikova EG, He Z, Patel T, Piroyan A, Sokolsky M, Kabanov AV, Batrakova EV (2015) Exosomes as drug delivery vehicles for Parkinson's disease therapy. J Control Release 207:18–30

Ishida T, Kashima S, Kiwada H (2008) The contribution of phagocytic activity of liver macrophages to the accelerated blood clearance (ABC) phenomenon of PEGylated liposomes in rats. J Control Release 126(2):162–165

Jiang XC, Gao JQ (2017) Exosomes as novel bio-carriers for gene and drug delivery. Int J Pharm 521(1–2):167–175

Johnsen KB, Gudbergsson JM, Skov MN, Pilgaard L, Moos T, Duroux M (2014) A comprehensive overview of exosomes as drug delivery vehicles - endogenous nanocarriers for targeted cancer therapy. Biochim Biophys Acta 1846(1):75–87

Kalani A, Kamat PK, Chaturvedi P, Tyagi SC, Tyagi N (2014) Curcumin-primed exosomes mitigate endothelial cell dysfunction during hyperhomocysteinemia. Life Sci 107(1–2):1–7

Kaur S, Singh SP, Elkahloun AG, Wu W, Abu-Asab MS, Roberts DD (2014) CD47-dependent immunomodulatory and angiogenic activities of extracellular vesicles produced by T cells. Matrix Biol 37: 49–59

Krausz AE, Adler BL, Makdisi J, Schairer D, Rosen J, Landriscina A, Navati M, Alfieri A, Friedman JM, Nosanchuk JD, Rodriguez-Gabin A, Ye KQ, McDaid HM, Friedman AJ (2018) Nanoparticle-encapsulated doxorubicin demonstrates superior tumor cell kill in triple negative breast Cancer subtypes intrinsically resistant to doxorubicin. Precis Nanomed 1(3):173–182

Lamichhane TN, Raiker RS, Jay SM (2015) Exogenous DNA loading into extracellular vesicles via electroporation is size-dependent and enables limited gene delivery. Mol Pharm 12(10):3650–3657

Liu C, Su C (2019) Design strategies and application progress of therapeutic exosomes. Theranostics 9(4):1015–1028

Long KB, Beatty GL (2013) Harnessing the antitumor potential of macrophages for cancer immunotherapy. Oncoimmunology 2(12): e26860

Maas SLN, Breakefield XO, Weaver AM (2017) Extracellular Vesicles: Unique Intercellular Delivery Vehicles. Trends Cell Biol 27(3):172–188

Mathivanan S, Ji H, Simpson RJ (2010) Exosomes: extracellular organelles important in intercellular communication. J Proteome 73(10): 1907–1920

Mendt M, Kamerkar S, Sugimoto H, McAndrews KM, Wu CC, Gagea M, Yang S, Blanko EVR, Peng Q, Ma X, Marszalek JR, Maitra A, Yee C, Rezvani K, Shpall E, LeBleu VS, Kalluri R (2018) Generation and testing of clinical-grade exosomes for pancreatic cancer. JCI Insight 3(8)

Mentkowski KI, Snitzer JD, Rusnak S, Lang JK (2018) Therapeutic potential of engineered extracellular vesicles. AAPS J 20(3):50

Mersin H, Yildirim E, Berberoglu U, Gulben K (2008) The prognostic importance of triple negative breast carcinoma. Breast 17(4):341–346

Mignot G, Roux S, Thery C, Segura E, Zitvogel L (2006) Prospects for exosomes in immunotherapy of cancer. J Cell Mol Med 10(2):376–388

Mohamed BM, Verma NK, Davies AM, McGowan A, Crosbie-Staunton K, Prina-Mello A, Kelleher D, Botting CH, Causey CP, Thompson PR, Pruijn GJ, Kisin ER, Tkach AV, Shvedova AA, Volkov Y (2012) Citrullination of proteins: a common post-translational modification pathway induced by different nanoparticles in vitro and in vivo. Nanomedicine (Lond) 7(8):1181–1195

Montecalvo A, Larregina AT, Shufesky WJ, Stolz DB, Sullivan ML, Karlsson JM, Baty CJ, Gibson GA, Erdos G, Wang Z, Milosevic J, Tkacheva OA, Divito SJ, Jordan R, Lyons-Weiler J, Watkins SC, Morelli AE (2012) Mechanism of transfer of functional microRNAs between mouse dendritic cells via exosomes. Blood 119(3):756–766

Morse MA, Garst J, Osada T, Khan S, Hobeika A, Clay TM, Valente N, Shreeniwas R, Sutton MA, Delcayre A, Hsu DH, Le Pecq JB, Lyerly HK (2005) A phase I study of dexosome immunotherapy in patients with advanced non-small cell lung cancer. J Transl Med 3(1):9

Mulcahy LA, Pink RC, Carter DR (2014) Routes and mechanisms of extracellular vesicle uptake. J Extracell Vesicles 3

Nordin JZ, Lee Y, Vader P, Mager I, Johansson HJ, Heusermann W, Wiklander OP, Hallbrink M, Seow Y, Bultema JJ, Gilthorpe J, Davies T, Fairchild PJ, Gabrielsson S, Meisner-Kober NC, Lehtio J, Smith CI, Wood MJ, Andaloussi SE (2015) Ultrafiltration with size-exclusion liquid chromatography for high yield isolation of

extracellular vesicles preserving intact biophysical and functional properties. Nanomedicine

Pachler K, Lener T, Streif D, Dunai ZA, Desgeorges A, Feichtner M, Oller M, Schallmoser K, Rohde E, Gimona M (2017) A good manufacturing practice-grade standard protocol for exclusively human mesenchymal stromal cell-derived extracellular vesicles. Cytotherapy 19(4):458–472

Pan Q, Ramakrishnaiah V, Henry S, Fouraschen S, de Ruiter PE, Kwekkeboom J, Tilanus HW, Janssen HL, van der Laan LJ (2012) Hepatic cell-to-cell transmission of small silencing RNA can extend the therapeutic reach of RNA interference (RNAi). Gut 61(9):1330–1339

Parolini I, Federici C, Raggi C, Lugini L, Palleschi S, De Milito A, Coscia C, Iessi E, Logozzi M, Molinari A, Colone M, Tatti M, Sargiacomo M, Fais S (2009) Microenvironmental pH is a key factor for exosome traffic in tumor cells. J Biol Chem 284(49):34211–34222

Patel S, Mehta-Damani A, Shu H, Le Pecq JB (2005) An analysis of variability in the manufacturing of dexosomes: implications for development of an autologous therapy. Biotechnol Bioeng 92(2):238–249

Peng Q, Zhang S, Yang Q, Zhang T, Wei XQ, Jiang L, Zhang CL, Chen QM, Zhang ZR, Lin YF (2013) Preformed albumin corona, a protective coating for nanoparticles based drug delivery system. Biomaterials 34(33):8521–8530

Pullan JE, Confeld MI, Osborn JK, Kim J, Sarkar K, Mallik S (2019) Exosomes as drug carriers for Cancer therapy. Mol Pharm 16(5):1789–1798

Raposo G, Stoorvogel W (2013) Extracellular vesicles: exosomes, microvesicles, and friends. J Cell Biol 200(4):373–383

Reis S, Lucio M, Segundo M, Lima JL (2010) Use of liposomes to evaluate the role of membrane interactions on antioxidant activity. Methods Mol Biol 606:167–188

Ren YX, Hao S, Jin X, Ye FG, Gong Y, Jiang YZ, Shao ZM (2019) Effects of adjuvant chemotherapy in T1N0M0 triple-negative breast cancer. Breast 43:97–104

Rice TF, Donaldson B, Bouqueau M, Kampmann B, Holder B (2018) Macrophage- but not monocyte-derived extracellular vesicles induce placental pro-inflammatory responses. Placenta 69:92–95

Rufino-Ramos D, Albuquerque PR, Carmona V, Perfeito R, Nobre RJ, Pereira de Almeida L (2017) Extracellular vesicles: novel promising delivery systems for therapy of brain diseases. J Control Release 262:247–258

Saleh AF, Lazaro-Ibanez E, Forsgard MA, Shatnyeva O, Osteikoetxea X, Karlsson F, Heath N, Ingelsten M, Rose J, Harris J, Mairesse M, Bates SM, Clausen M, Etal D, Leonard E, Fellows MD, Dekker N, Edmunds N (2019) Extracellular vesicles induce minimal hepatotoxicity and immunogenicity. Nanoscale 11(14):6990–7001

Schindler C, Collinson A, Matthews C, Pointon A, Jenkinson L, Minter RR, Vaughan TJ, Tigue NJ (2019) Exosomal delivery of doxorubicin enables rapid cell entry and enhanced in vitro potency. PLoS One 14(3):e0214545

Sena-Esteves M, Tebbets JC, Steffens S, Crombleholme T, Flake AW (2004) Optimized large-scale production of high titer lentivirus vector pseudotypes. J Virol Methods 122(2):131–139

Shtam TA, Kovalev RA, Varfolomeeva EY, Makarov EM, Kil YV, Filatov MV (2013) Exosomes are natural carriers of exogenous siRNA to human cells in vitro. Cell Commun Signal 11:88

Singhto N, Kanlaya R, Nilnumkhum A, Thongboonkerd V (2018) Roles of macrophage Exosomes in immune response to calcium oxalate monohydrate crystals. Front Immunol 9:316

Sorolla A, Wang E, Clemons TD, Evans CW, Plani-Lam JH, Golden E, Dessauvagie B, Redfern AD, Swaminathan-Iyer K, Blancafort P (2019) Triple-hit therapeutic approach for triple negative breast cancers using docetaxel nanoparticles, EN1-iPeps and RGD peptides. Nanomedicine

Sun D, Zhuang X, Xiang X, Liu Y, Zhang S, Liu C, Barnes S, Grizzle W, Miller D, Zhang HG (2010) A novel nanoparticle drug delivery system: the anti-inflammatory activity of curcumin is enhanced when encapsulated in exosomes. Mol Ther 18(9):1606–1614

Taheri, B., M. Soleimani, S. Fekri Aval, E. Esmaeili, Z. Bazi and N. Zarghami (2018). "Induced pluripotent stem cell-derived extracellular vesicles: A novel approach for cell-free regenerative medicine." J Cell Physiol

Tian Y, Li S, Song J, Ji T, Zhu M, Anderson GJ, Wei J, Nie G (2014) A doxorubicin delivery platform using engineered natural membrane vesicle exosomes for targeted tumor therapy. Biomaterials 35(7):2383–2390

Valcourt, D. M., M N Dang and E. S. Day (2019). "IR820-loaded PLGA nanoparticles for photothermal therapy of triple-negative breast cancer." J Biomed Mater Res A

Veronese FM, Caliceti P, Schiavon O, Sergi M (2002) Polyethylene glycol-superoxide dismutase, a conjugate in search of exploitation. Adv Drug Deliv Rev 54(4):587–606

Wahlgren J, De LKT, Brisslert M, Vaziri Sani F, Telemo E, Sunnerhagen P, Valadi H (2012) Plasma exosomes can deliver exogenous short interfering RNA to monocytes and lymphocytes. Nucleic Acids Res 40(17):e130

Walsh EM, Shalaby A, O'Loughlin M, Keane N, Webber MJ, Kerin MJ, Keane MM, Glynn SA, Callagy GM (2019) Outcome for triple negative breast cancer in a retrospective cohort with an emphasis on response to platinum-based neoadjuvant therapy. Breast Cancer Res Treat 174(1):1–13

Yoshida K, Burton GF, McKinney JS, Young H, Ellis EF (1992) Brain and tissue distribution of polyethylene glycol-conjugated superoxide dismutase in rats. Stroke 23(6):865–869

Yuan D, Zhao Y, Banks WA, Bullock KM, Haney M, Batrakova E, Kabanov AV (2017) Macrophage exosomes as natural nanocarriers for protein delivery to inflamed brain. Biomaterials 142:1–12

Zhang Y, Liu Y, Liu H, Tang WH (2019) Exosomes: biogenesis, biologic function and clinical potential. Cell Biosci 9:19

Zhou Q, Ji M, Zhou J, Jin J, Xue N, Chen J, Xu B, Chen X (2016) Poly (ADP-ribose) polymerases inhibitor, Zj6413, as a potential therapeutic agent against breast cancer. Biochem Pharmacol 107:29–40

Zhuang X, Xiang X, Grizzle W, Sun D, Zhang S, Axtell RC, Ju S, Mu J, Zhang L, Steinman L, Miller D, Zhang HG (2011) Treatment of brain inflammatory diseases by delivering exosome encapsulated anti-inflammatory drugs from the nasal region to the brain. Mol Ther 19(10):1769–1779